SCIENTIFIC ARTICLE

Non-coding RNA Identification in Osteonecrosis of the Femoral Head Using Competitive Endogenous RNA Network Analysis

Ning Han, MD Zengchun Li, MD

Department of Emergency Trauma Surgery, Shanghai East Hospital of Tongji University, Shanghai, China

Objective: To investigate the regulatory network of long non-coding RNA (lncRNA) as competing endogenous RNAs (ceRNAs) in osteonecrosis of the femoral head (ONFH).

Methods: The gene expression profile GSE74089 of ONFH and microRNA (miRNA) expression profile of GSE89587 were obtained from the Gene Expression Omnibus (GEO) database. The GSE74089 contained four ONFH samples and four controls. The GSE89587 included 10 ONFH samples and 10 control samples. The differentially expressed lncRNAs (DE-lncRNAs) and DE-mRNAs between ONFH group and control group were identified from GSE74089 using the limma package based on criteria of adjusted P value <0.05 and |log fold change (FC)| ≥2. The DEmiRNAs between ONFH group and control group were screened from GSE89587 on the basis of adjusted P value <0.05. Gene ontology (GO) and Kyoto Encyclopedia of Genes and Genomes (KEGG) pathway for DE-mRNAs were analyzed using DAVID 6.7 and GSEA 3.0, respectively. Coexpressed lncRNA-mRNA pairs were identified by corr.test method in R based on the criteria of adjusted P value <0.01 and $|r|$ ≥ 0.9. A ceRNA network was constructed and visualized using cytoscape 3.7.0 by integrating the DE-lncRNA, DE-miRNA, and DEmRNA data. The key mRNAs and lncRNAs in the ceRNA network were further validated in an independent dataset of GSE123568.

Results: Based on our analysis, a total of 28 DE-lncRNAs, 1403 DE-mRNAs, and 134 DE-miRNAs were identified, respectively. The DE-mRNAs were significantly enriched in the function of "skeletal system development," "collagen fibril organization," "blood vessel development," and "regulation of nervous system development." Besides, 72 KEGG pathways, including eight active pathways and 64 suppressed pathways were identified, including which immune pathway was the most significantly activated one and which ribosome-related function was the most suppressed. A co-expression network including 161 DE-mRNAs and 16 DE-lncRNAs was built. Highly connected nodes were identified among lncRNAs such as *H19*, *C20orf203*, *LINC00355*, *SFTA3*, *CRNDE*, *CASC2*, *LINC00494*, *C9orf163*, *C10orf91*, and *LINC00301*. The ceRNA network indicated that lncRNA *H19* functioned as a ceRNA of hsa-miR-519b-3p and hsa-miR-296-5p in *ANKH* and *ECHDC1* regulation; lncRNA *C9orf163* functioned as a ceRNA of hsa-miR-424-5p in *CCNT1* regulation. The expression trends of *ANKH*, *CCNT1*, and *C9orf163* were successfully validated in independent dataset of GSE123568.

Conclusion: The ceRNAs of lncRNA *H19*- hsa-miR-519b-3p/hsa-miR-296-5p-*ANKH* and lncRNA *c9orf163*- hsa-miR-424-5p-*CCNT1* might play important roles in ONFH development. Our research provided an understanding of the important role of lncRNA–related ceRNAs in ONFH.

Key words: Competing endogenous RNAs; Long non-coding RNA; Osteonecrosis of the femoral head

Introduction

Osteonecrosis of the femoral head (ONFH) is a devastating condition that affects patients for about 30 to 50 years of life and usually progresses to femoral collapse[1]. About 20,000 to 30,000 new adults will be diagnosed in the United States annually[2]. Different etiologies participate in the ONFH. The femoral neck fracture or dislocation of the femoral head is one of the most common causes. Besides, autoimmune and chronic inflammatory disorders, long-term steroid treatment, and vascular damage were reported in the development of ONFH[3]. ONFH is a multifactorial disease that involves multiple factors. Several proteins have been identified in the progression of ONFH including lipoprotein, p-glycoprotein, zinc-α2-glyoprotein, glycoprotein-39, vascular endothelial growth factor (VEGF). There is research that provides pharmaceutical incidence[4, 5]. But the exact mechanism has not been fully delineated. Fully understanding the mechanism allows earlier treatment of ONFH and potentially improves the outcome.

Recently, non-coding RNAs (ncRNAs) have been reported to illustrate their function in various diseases. The long-non coding RNA (lncRNA) is one type of ncRNAs that showed regulatory function in various human diseases[6]. Recent studies have identified several lncRNAs that play important roles in ONFH. For example, Wang et al. investigated the lncRNA expression profile of bone marrow mesenchymal stem cells of steroid induced ONFH patients for the first time and identified lncRNA RP1-193H18.2, Metastasis Associated Lung Adenocarcinoma Transcript 1 (MALAT1) and HOX Transcript Antisense RNA (HOTAIR) were associated with the abnormal osteogenic differentiation in ONFH patients[6]. Xiang et al. demonstrated that lncRNA RP11-154D6 could promote osteogenic differentiation while inhibiting adipogenic differentiation in ONFH patients[7]. Huang et al. demonstrated that lncRNA family with sequence similarity 201-member A (FAM201A) was downregulated in ONFH patients and its downregulation was correlated with the development of ONFH[8]. Chen et al. demonstrated that lncRNA AWPPH was significantly downregulated in non-traumatic ONFH patients and may upregulate Runx2 to participate in the development of ONFH[9].

MicroRNA (miRNA) is another important type of ncRNA. Previous research has indicated that miRNAs play crucial roles in diverse physiological process and participate in the process of osteogenesis including osteoclast formation, differentiation, apoptosis, and resorption[10–12]. Increasing evidence has suggested the critical roles of several miRNAs in regulating bone development[13–15]. With the assistance of high-throughput technology, such as microarray and RNA sequencing, more and more miRNAs have been reported to be important in the development of ONFH[16, 17]. A total of 12 upregulated miRNAs and five dowregulated miRNAs were identified by microarry in ONFH tissues compared with control tissues[18]. Similarly, Wu et al. identified 22 upregulated miRNAs and 17 downregulated miRNAs between four non-traumatic ONFH and four femoral neck fractures[16]. In a cell model of ONFH, Bian et al. identified 17 altered miRNAs in mesenchymal stem cells treated with dexamethasone[19]. However, the molecular mechanisms of most of these miRNAs generated by high-throughput technology were not investigated in detail.

In recent years, more and more studies showed that the lncRNAs could target miRNA and regulate gene expression indirectly[20]. This kind of lncRNA was defined as acting as competing endogenous RNAs (ceRNAs), which indicated the lncRNAs competed for binding to miRNAs with mRNAs to regulate the target gene expression. Wei et al. demonstrated that lncRNA HOTAIR might function as a ceRNA to regulate expression of Family Member 7 (SMAD7) by sponging miRNA-17-5p in non-traumatic ONFH[21]. Several lncRNAs acting as ceRNAs have been reported in cancers[22]. However, the lncRNAs that function as ceRNAs in the ONFH has not been investigated in detail.

In this study, we aimed to: (i) analyze gene expression data of ONFH; (ii) identify critical lncRNAs and mRNAs involved in the development of ONFH; (iii) decipher the regulatory ceRNA network of lncRNAs–miRNAs–mRNAs in ONFH. The flow chart of this study is shown in Fig. 1. This study might be helpful to explore the molecular mechanisms of ONFH.

Materials and Methods

Data Source

The microarray data of expression profile of GSE74089 (GPL13497) was obtained from the National Center for Biotechnology Information (NCBI) GEO database[23]. The GSE74089 was obtained from GLP13974 (Agilent-026652 Whole Human Genome Microarray 4 × 44K v2) with samples from four ONFH patients and four controls[24]. miRNA microarray expression profile GSE89587 (GPL18402, Agilent-046064 Unrestricted_Human_miRNA_V19.0_Microarray) from 10 ONFH samples and 10 control samples was also obtained[25]. In these datasets, annotation "protein_coding" was defined as mRNA, "antisense, sense_intronic, lincRNA, sense_overlapping, processed_transcript, 3′ overlapping_ncRNA, non_coding" were defined as ncRNA.

The dataset of GSE123568 was downloaded from GEO database as validation dataset. This dataset was deposited by Zhang et al. and included microarray data from 30 steroid-induced ONFH patients and 10 non-steroid-induced ONFH patients[26]. The platform of this dataset was GPL15207 ([PrimeView] Affymetrix Human Gene Expression Array).

Differential Expression Analysis

Differentially expressed lncRNAs (DE-lncRNAs) and DE-mRNAs were identified from the gene expression profile of GSE74089 using the limma package (version 3.10.3) in R[27]. Differentially expressed miRNAs (DE-miRNAs) were identified from the miRNA microarray expression profile GSE89587. The P value was adjusted using the Benjamini–Hochberg method. DE-lncRNAs and DE-mRNAs were filtered with the adjusted P value <0.05 and |log fold change
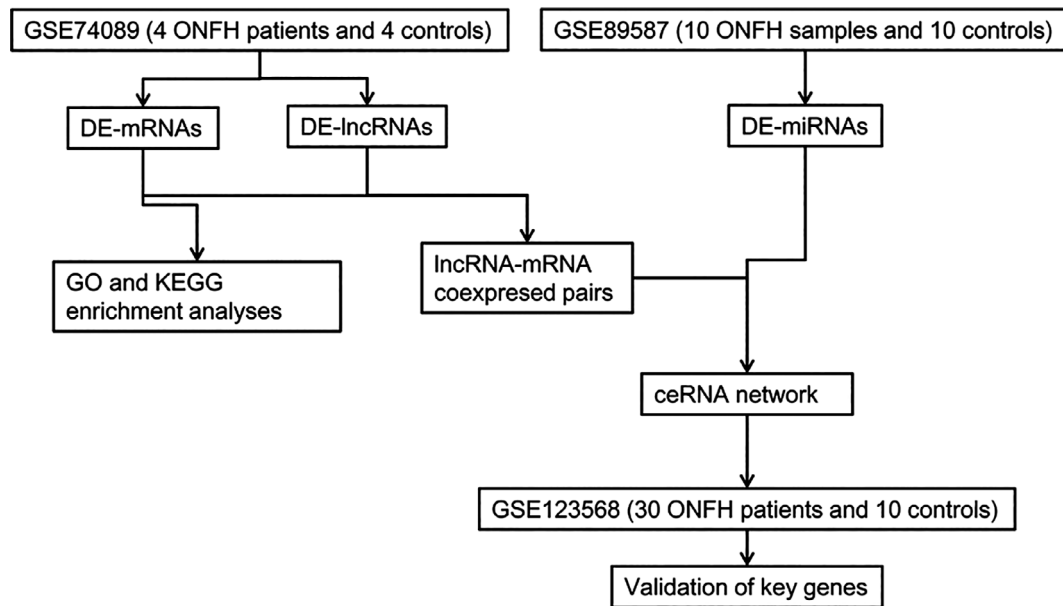
Fig. 1 The flow chart of the whole study.

(FC)| ≥2, while DE-miRNAs was screened based on the criterion of adjusted P value <0.05.

Functional Enrichment Analysis
The Gene Ontology analysis of DE-mRNAs was performed using DAVID version 6.7 and visualized by GOplot in R^{28}.

KEGG pathway enrichment of DE-mRNAs was implemented using Gene set enrichment analysis version 3.0 (GSEA) with the adjusted P value <0.05[29]. The pathways with Normalized Enrichment Score (NES) larger than 0 indicated the pathways were activated while NES smaller than 0 indicated the pathways were suppressed.

CeRNA Network Construction
Pearson's correlation coefficients (PCC) between DE-lncRNAs and DE-mRNAs were calculated using psych package in R with corr.test method (ci = F, adjust="BH"). Cytoscape (version 3.7.0) was used for visualization of the coexpressed lncRNA-mRNA pairs with adjusted P value <0.01 and $|r| ≥ 0.9$ [30].

The ceRNA network was constructed under the following procedures: (i) the interactions between DE-lncRNAs and DE-miRNAs were predicted using starbase database[31]; (ii) the interactions between DE-miRNAs and DE-mRNAs were predicted using miRTarBase, miRDB, and TargetScan and VENN diagram was used to filter out the miRNA-mRNA pairs localized in at least two of the three databases; (iii) the co-expressed DE-lncRNAs and DE-mRNAs that were regulated by same DE-miRNA and the expression patterns of DE-miRNA in ONFH was opposite (lncRNA and mRNA were upregulated in ONFH, while miRNA was

downregulated in ONFH or lncRNA, and mRNA were downregulated in ONFH, while miRNA was upregulated in ONFH) with DE-lncRNAs and DE-mRNAs used for constructing ceRNA network by Cytoscape.

Validation of Key Genes in the ceRNA Network
The key mRNAs and lncRNAs in the ceRNA network were further validated in an independent dataset of GSE123568. The differential expression of these mRNAs and lncRNAs were compared using Welch's non-paired t test. $P < 0.05$ was regarded as the statistical significant level.

Results

DEGs Identification in ONFH Samples
There were 17,372 mRNAs and 395 ncRNAs in GSE74089 dataset. There were 1153 miRNAs in the dataset GSE89587. A total of 1403 DE-mRNAs, 28 DE-lncRNAs, and 134 DE-miRNAs were identified, in which 378 mRNAs, 15 lncRNAs, and 59 miRNAs were up-regulated; 1025 mRNAs, 13 lncRNAs, and 75 miRNAs were down-regulated. Volcano plots revealed that mRNAs, lncRNAs, and miRNAs were differentially expressed between ONFH patients and control subjects (Fig. 2A,C,E) and the top 10 up-regulated and down-regulated genes were illustrated in heatmap (Fig. 2B,D,F).

GO Enrichment Analysis
To explore the biological function of these DE-mRNAs, GO enrichment analysis was performed. As a result, 18 GO terms including nine biological process (BP) functions and nine cellular component (CC) functions were significantly
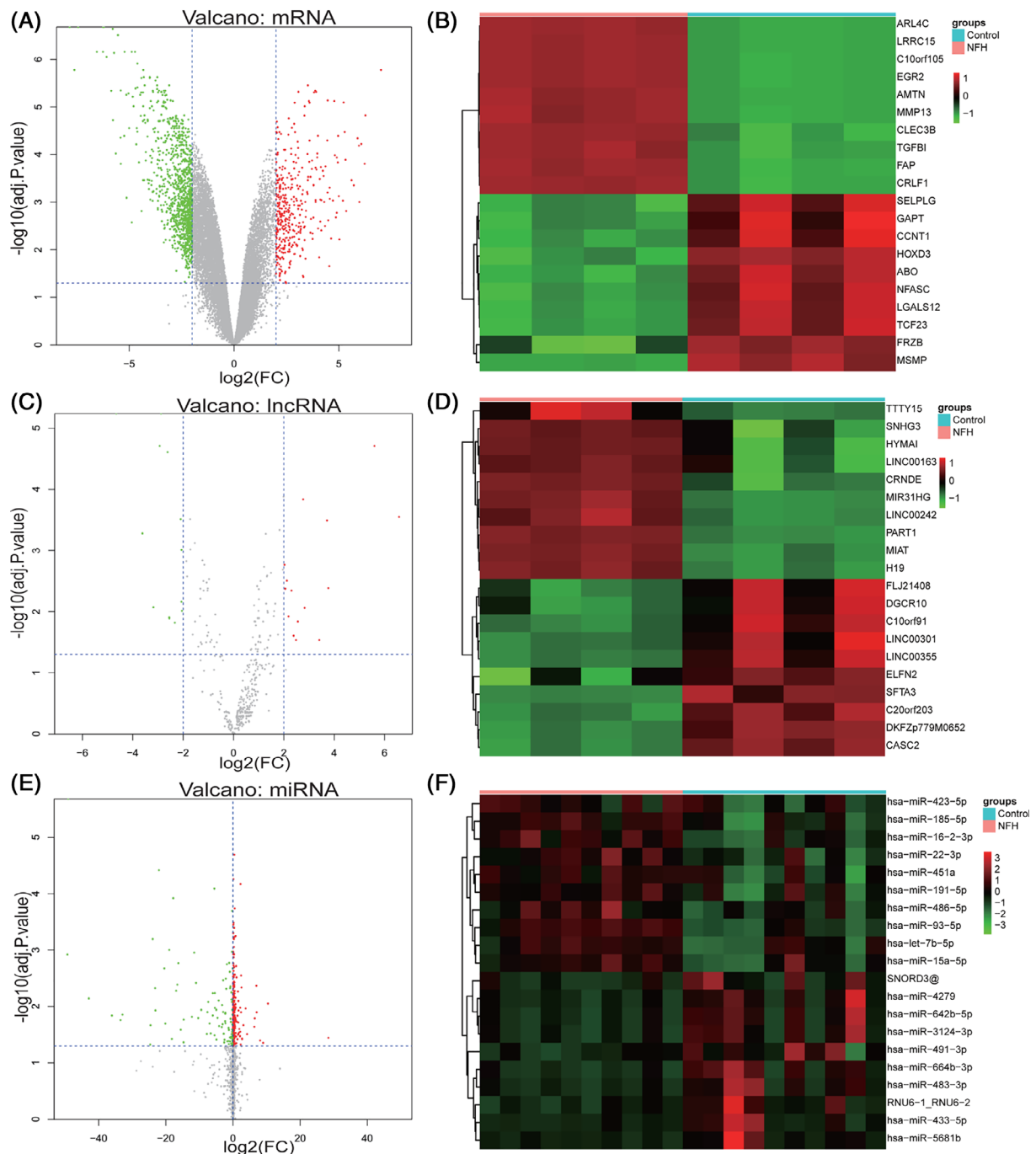
Fig. 2 Differentially expressed genes (DEGs) identification between osteonecrosis of the femoral head (ONFH) and normal samples. The DE-lncRNAs and DE-mRNAs between ONFH and normal samples were identified from GSE74089 by limma package in R based on the criteria of with the adjusted *P* value <0.05 and |log fold change (FC)| ≥2. DE-miRNAs were identified from GSE89587 on the basis of adjusted *P* value <0.05. Volcano plots display the distribution of DE-mRNAs (A), DE-lncRNAs (C), and DE-miRNAs (E). The vertical dotted lines in A and C represent |log FC| = 2 and the horizontal dotted lines represent adjusted *P* value = 0.05. Red spots represent up-regulated genes and green spots represent down-regulated genes in ONFH samples compared with normal samples. Hierarchical clustering demonstrates the top 10 DE-mRNAs (B), DE-lncRNAs (D), and DE-miRNAs (F) in descending order by log FC.

enriched (Fig. 3). The significant GO-BPs included "skeletal system development" (*P* value = 4.82E-07), "collagen fibril organization" (*P* value = 2.25E-06), and "blood vessel development" (*P* value = 1.51E-05). GO-CC analysis illustrated that the DE-mRNAs were mainly located in "extracellular region" (*P* value = 1.20E-10), "proteinaceous extracellular matrix" (*P* value = 3.86E-10), "collagen" (*P* value = 8.81E-07), "fibrillar collagen" (*P* value = 8.23E-06), and "Golgi membrane" (*P* value = 1.06E-06). These results revealed that these genes functioned in skeletal development, collagen fibril organization, and blood vessel development.

KEGG Enrichment

Next, KEGG pathway enrichment was performed and 72 pathways were identified, in which eight pathways were activated (NES > 0) and 64 pathways were suppressed (NES < 0, Fig. 4A,B). Among the active pathways, "intestinal immune network for IgA production" (*P* value = 0.009), "allograft rejection" (*P* value = 0.007), and "*Staphylococcus aureus* infection" (*P* value = 0.004) were the most significantly activated pathways (Fig. 4C). The suppressed pathways included "hippo signaling pathway" (*P* value = 0.001), "TGF-beta signaling pathway" (*P* value = 0.004), "p53 signaling pathway" (*P* value = 0.008), "mTOR signaling pathway" (*P* value = 0.008), and "PI3K-AKT signaling pathway" (*P* value = 0.002). Among these, "ribosome" (*P* value = 0.001) was the most significantly suppressed pathway (Fig. 4D). The top 10 significant suppressed pathways and the eight activated pathways are shown in the Supplementary Table S1.
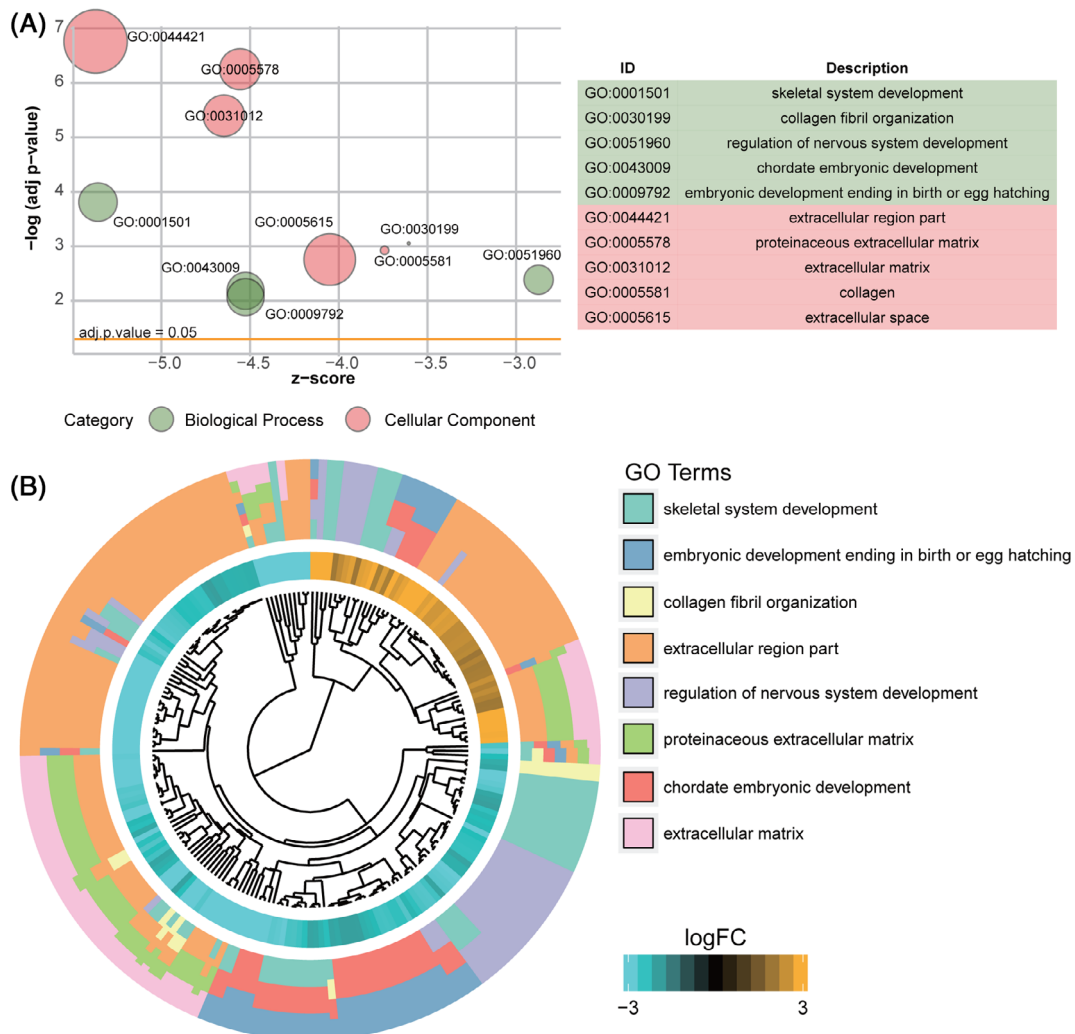

Fig. 3 Gene Ontology (GO) enrichment analysis of DE-mRNAs. The GO enrichment analysis was performed using DAVID and visualized by GOplot in R. (A) The top five bubble plot of GO terms. X-axis represents the Z-score and Y-axis represents the negative log (adjusted *P* value). The area of the bubble positively correlates with the gene numbers in the indicated term. The green represents the GO-biological process terms and the pink represents the GO-cellular component terms. (B) GO cluster of genes in the top eight GO terms grouped by their expression level.
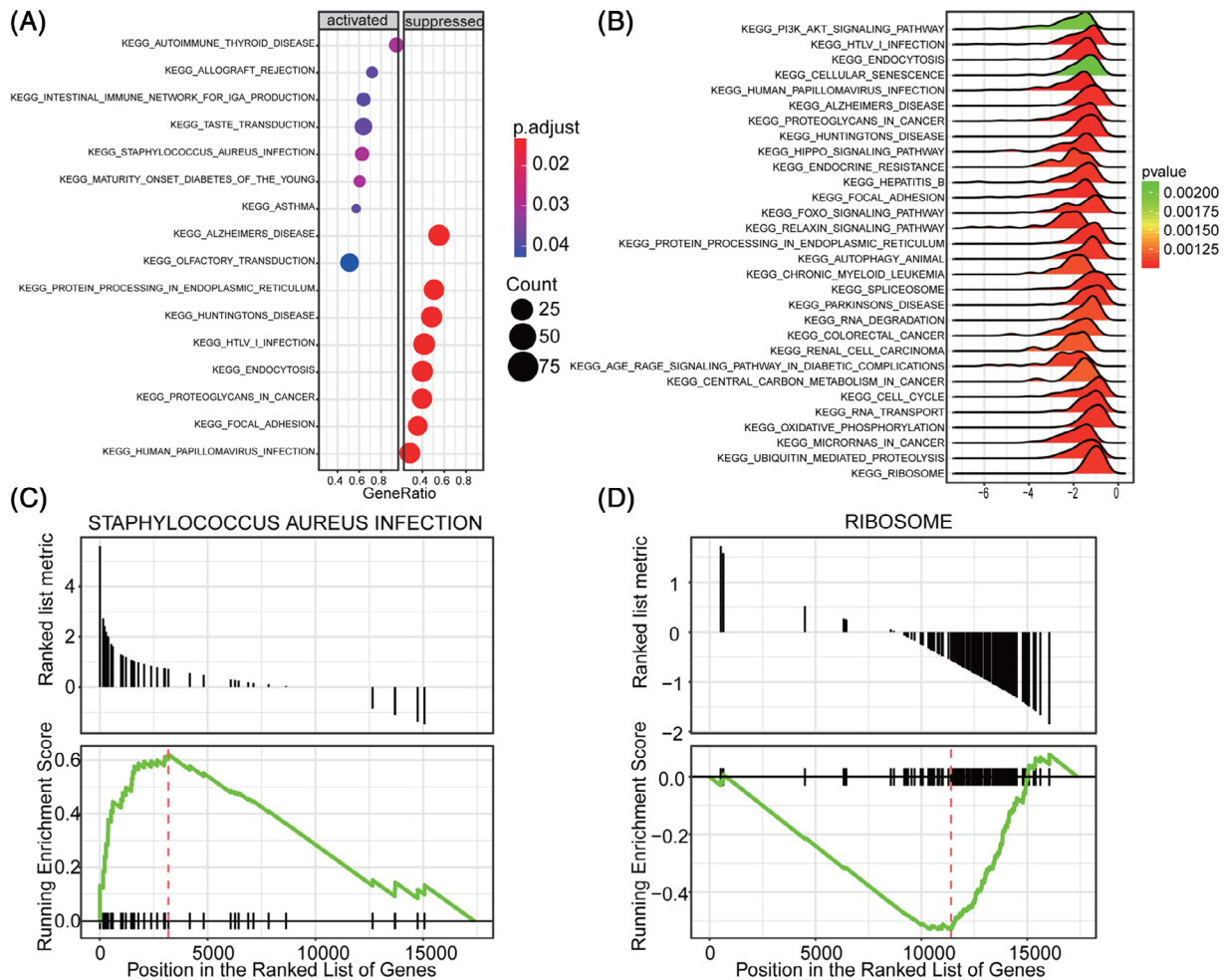
Fig. 4 KEGG pathway enrichment analysis of DE-mRNAs. The KEGG pathway enrichment of DE-mRNAs was performed by Gene set enrichment analysis. (A) Dot plot of dysregulated pathways in ONFH samples compared with normal samples. The color intensity of the nodes indicates KEGG pathways enrichment degree. Horizontal axis indicates the gene ratio as the proportion of differential genes in the whole gene set. The size represents the number counts in a certain pathway. (B) Ridge plot of dysregulated pathways. The colored intensity of peaks indicates enrichment significance. Horizontal axis represents *P* value. (C, D) Genes involved in *Staphylococcus aureus* infection pathway and ribosome pathway. Running enrichment score was negative for most genes in *Staphylococcus aureus* infection pathway and positive for most genes in ribosome pathway.

LncRNA-mRNA Co-expressed Network and ceRNA Network Construction

Next, DE-mRNAs and DE-lncRNAs were used to construct a co-expression network (Fig. 5). There were 177 nodes and 175 edges in the co-expression network including 161 DE-mRNAs and 16 DE-lncRNAs. Highly connected nodes were identified among lncRNAs such as *H19 Imprinted Maternally Expressed Transcript (H19), Chromosome 20 Open Reading Frame 203 (C20orf203), long intergenic non-protein coding RNA 355 (LINC00355), Surfactant Associated 3 (SFTA3), Colorectal Neoplasia Differentially Expressed (CRNDE), Cancer Susceptibility 2 (CASC2), long intergenic non-protein coding RNA 494 (LINC00494), Chromosome 9 Open Reading Frame 163 (C9orf163), Chromosome 10 Open Reading Frame 91 (C10orf91)* and *long intergenic non-protein coding RNA 301 (LINC00301).*

CeRNA Network Construction

The miRNA-mRNA interactions were predicted in Targetscan, miRDB, and miRTarBase. The miRNA-mRNA interactions that were predicted in at least two databases were selected for further analysis. Based on the intersection elements, 240 miRNA-mRNA pairs were identified (Fig. 6A). Meanwhile, the lncRNA targeted by miRNA were predicted using starBase database and 10 lncRNAs were identified: *H19, C20orf203, LINC00355, SFTA3, CRNDE, CASC2, LINC00494, C9orf163, C10orf91,* and *LINC00301.* After integrating miRNA-lncRNA pairs and miRNA-mRNA pairs, a ceRNA network was constructed (Fig. 6B). This ceRNA network included three DE-mRNAs: Ethylmalonyl-CoA Decarboxylase 1 (*ECHDC1*), Ankylosis protein homolog human gene (*ANKH*), and Cyclin T1 (*CCNT1*); three DE-miRNAs: hsa-miR-519b-3p,
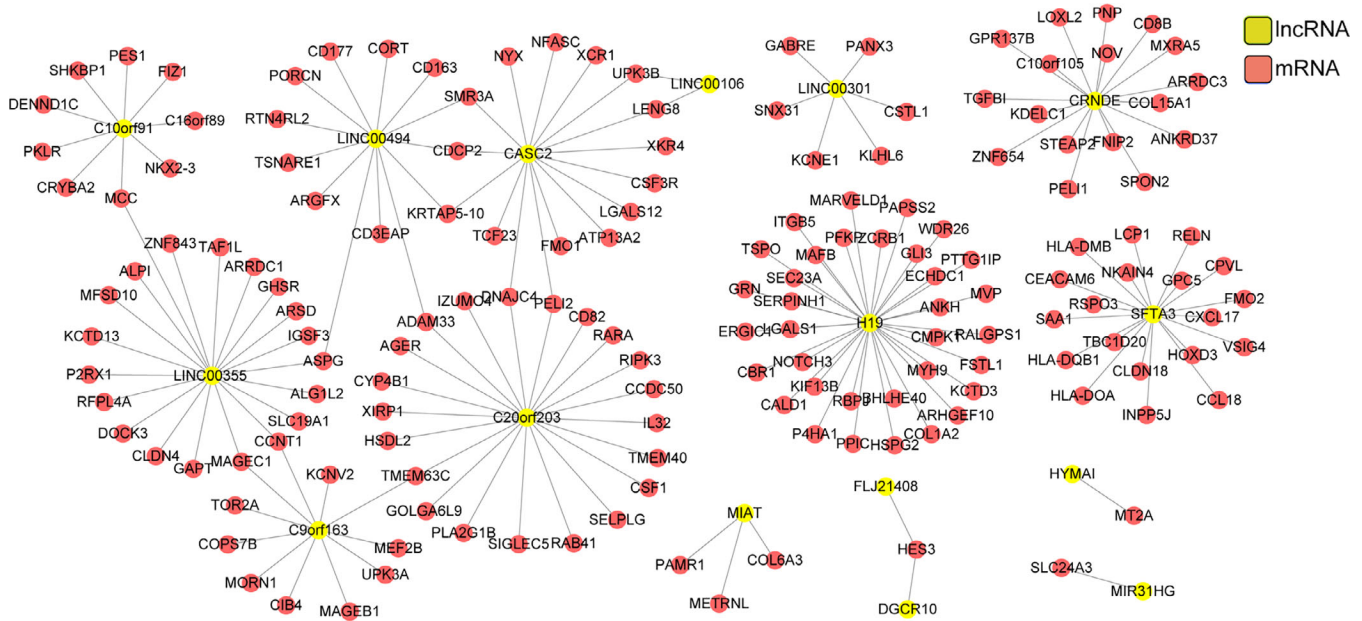
Fig. 5 ncRNA-mRNA coexpression network constructed using DE-mRNAs and DE-lncRNAs. Pearson's correlation coefficients (PCC) between DE-lncRNAs and DE-mRNAs were calculated using psych package in R and the coexpressed lncRNA-mRNA pairs with adjusted *P* value <0.01 and |r| ≥ 0.9 were visualized by Cytoscape. Gene pairs were chosen using correlation ratio |r| ≥ 0.9 and adj. *P* value <0.05. red, mRNA; yellow, ncRNA.
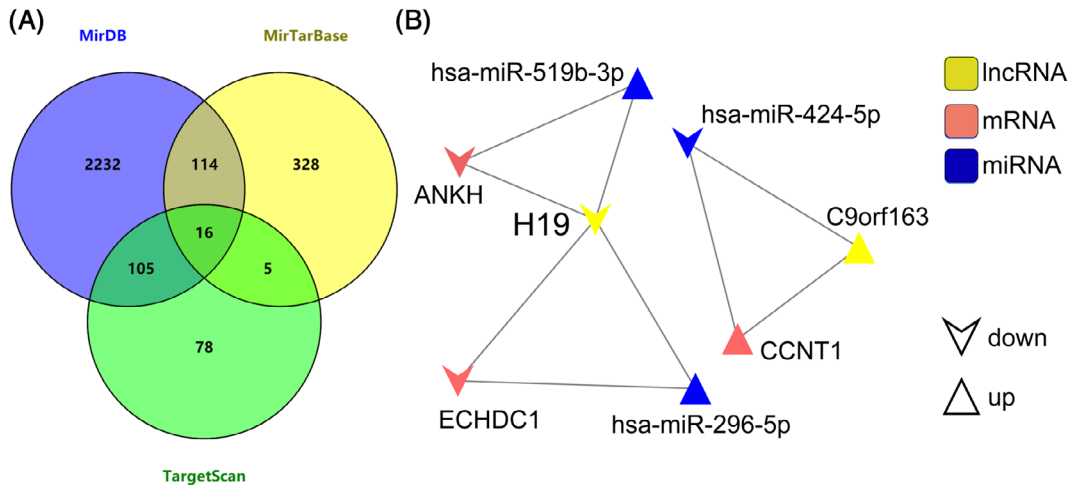

Fig. 6 CeRNA network construction. The co-expressed DE-lncRNAs and DE-mRNAs that were regulated by same DE-miRNA and the expression patterns of DE-miRNA in ONFH was opposite with DE-lncRNAs and DE-mRNAs used for constructing ceRNA network by Cytoscape. (A) Venn diagram shows the number of predicted miRNA-mRNA interactions from mirDB, mirTraBase, and TargetScan. (B) ceRNA network. Pink nodes were mRNAs, yellow nodes were lncRNAs, and blue nodes were miRNAs.

hsa-miR-424-5p, hsa-miR-296-5p; and two DE-lncRNAs: *H19* and *C9orf163*. As shown in the ceRNA network, lncRNA *H19* might function as a ceRNA of hsa-miR-519b-3p and hsa-miR-296-5p to enhance the expression of *ECHDC1* and *ANKH* in ONFH. LncRNA *C9orf163* might target hsa-miR-296-5p and then regulate the expression of *CCNT1*.

Validation of Key Genes in the ceRNA Network
The three key mRNAs (*ECHDC1*, *ANKH*, and *CCNT1*) and two lncRNAs (*H19* and *C9orf163*) in the ceRNA network were further validated in an independent dataset of GSE123568. Because of the different platforms of the original dataset of GSE74089 and the validation dataset of
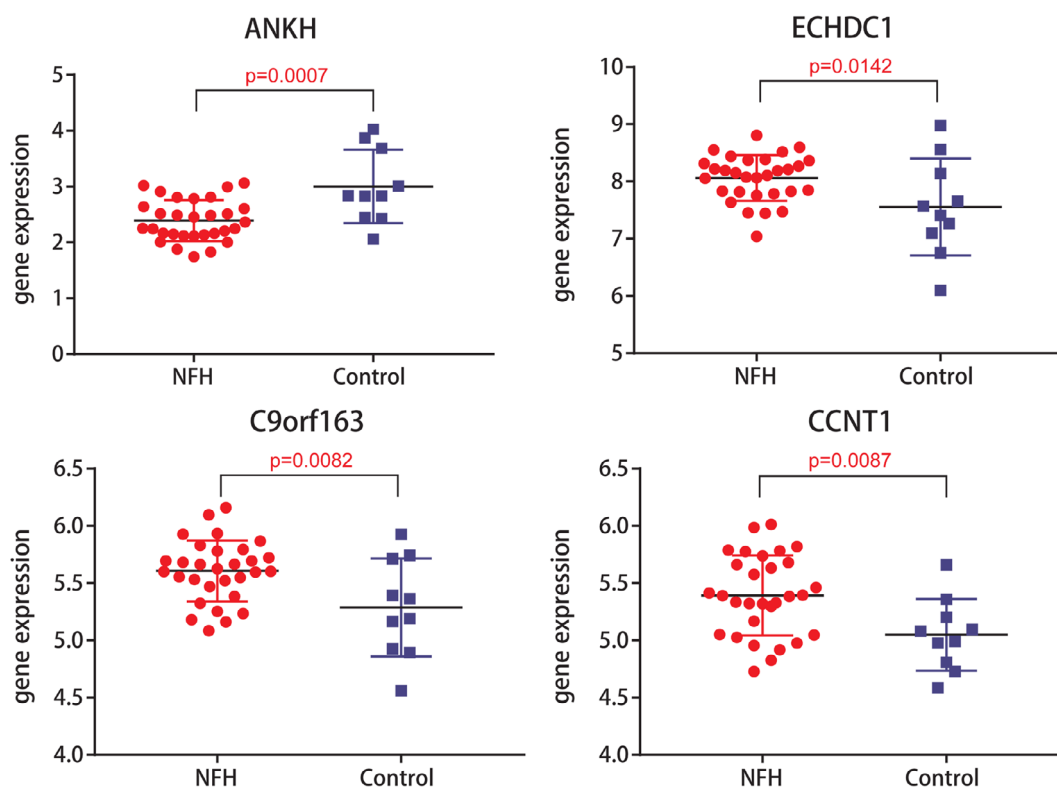
Fig. 7 Validation of key lncRNAs and mRNAs in an independent dataset. The key mRNAs and lncRNAs in the ceRNA network were validated in an independent dataset of GSE123568. The differential expression of these mRNAs and lncRNAs were compared using Welch's non-paired t test. *P* < 0.05 was regarded as the statistically significant level.

GSE123568, the lncRNA *H19* was not detected in the dataset of GSE123568. The differential expression of *ECHDC1*, *ANKH*, *CCNT1*, and *C9orf163* between ONFH samples and control samples is shown in Fig. 7. All of these four genes were significantly differentially expressed between ONFH samples and control samples. Among them, the expression trends of *ANKH*, *CCNT1*, and *C9orf163* were consistent with the original dataset, while the expression trend of *ECHDC1* was opposite the original dataset. The successful rate of validation is 75%, suggesting a relatively high reliability of the results.

Discussion

ONFH is usually induced by the destruction of the blood supply and the coagulation and fibrinolysis system disorder[32]. However, the specific molecular mechanism of ONFH is unclear. In this study, we found DE-mRNAs were mainly functioned in skeletal system, blood vessel development. Further, we found the immune system might function in the ONFH development. Co-expression network analysis revealed several key lncRNAs played roles in ONFH development such as *H19*, *C20orf203*, *LINC00355*, *SFTA3*, *CRNDE*, *CASC2*, *LINC00494*, *C9orf163*, *C10orf91*, and *LINC00301*. Then, we first performed a miRNA-lncRNA-mRNA ceRNA network construction, in which two lncRNAs *H19* and

C9orf163 mainly targeted hsa-miR-519b-3p, hsa-miR-424-5p, and hsa-miR-296-5p and then regulated the expression of *ECHDC1*, *ANKH*, and *CCNT1*. Among them, the differential expression of *ANKH*, *CCNT1*, and *C9orf163* was successfully validated in an independent dataset.

Previous research has illustrated multiple biological processes were involved in the development of ONFH. Circulation, steroid metabolism, immunity, and bone formation have been reported as the etiologies of ONFH[33]. Immune disorder was associated with ONFH and several genes involved in immunity have shown correlation with ONFH. For example, the rs1800587 SNP of interleukin (IL)-1α has revealed increased risk of ONFH[34]. Besides, *IL-23* and *IL-33* have shown their predictive value of ONFH[35, 36]. The SNP of Tumor Necrosis Factor-α (*TNF-α*) gene showed their association with ONFH[37]. In this study, we found the DE-mRNAs were significantly enriched in immune-related pathways, such as "intestinal immune network for IgA production" and "allograft rejection," and might function in the development of ONFH, which was consistent with previous research.

Recently, emerging evidence provided a novel regulatory mechanism between miRNA and lncRNA. LncRNAs could act as miRNA sponges to regulate the expression of miRNA target genes and participate in multiple biological processes. But the lncRNA-miRNA regulatory network in ONFH has not been

fully illustrated. ncRNAs have shown their incidence in the pathogenesis of ONFH. Several studies have suggested that miRNAs have been critically investigated and showed their important roles in the development of ONFH. MiR-146a and miR-34a were up-regulated in the ONFH[16]. Circulating miRNAs were used as markers for ONFH diagnosis. Up-regulated miR-10a-5p and down-regulated miR-423-59 were confirmed in ONFH[34]. Functional significance of up-regulated miR-708, miR-210 and down-regulated miR-548d-5p, miR-17-5p, miR-27a were found in ONFH patients[38–41]. It has been reported that lncRNAs of *CRNDE, CASC2, RP11-154D6, Myocardial Infarction Associated Transcript* (*MIAT*), *RP1-193H18.2, MALAT1*, and *HOTAIR* have shown their correlations with ONFH[6, 7, 42, 43]. In our research, we identified the 10 lncRNAs of *H19, C20orf203, LINC00355, SFTA3, CRNDE, CASC2, LINC00494, C9orf163, C10orf91*, and *LINC00301* in the development of ONFH. Among these, *CRNDE* and *CASC2* have been identified before in ONFH[43, 44].

In the present study, we constructed a ceRNA network and several ceRNA relationships among lncRNAs, miRNAs, and mRNAs were identified. For example, we found the lncRNA *H19* could bind to hsa-miR-519b-3p and hsa-miR-296-5p to regulate the expression of *ECHDC1* and *ANKH*. Also, we found the lncRNA *c9orf163* could up-regulate *CCNT1* by sponging hsa-miR-424-5p.

It is well known that *H19* is an imprinted gene, and *H19* is re-expressed in a wide variety of tumor types and as tumor-suppressed genes[45]. In non-small cell lung cancer, miR-296-5p suppresses cell viability[46]. In muscle-wasting patients, rRNA synthesis is inhibited by miR-424-5p regulation in pol I pre-initiation complex formation[47]. Decreased expression of miR-519b-3p was observed in colorectal cancer, which indicated the suppressed invasion and proliferation function in colorectal cancer cells[48]. Ethylmalonyl-CoA decarboxylase (*ECHDC1*) has shown its function in bladder cancer, breast cancer, and ovarian cancer[49]. Ankylosis protein homolog human gene (*ANKH*) mutations have been reported in inherited human disorders such as familial calcium pyrophosphate deposition disease (CPPD) and cranial metaphyseal dysplasia[50]. But the roles of the following have not been revealed before: lncRNA of *H19*; miRNAs of hsa-miR-519b-3p, hsa-miR-296-5p and hsa-miR-424-5p; mRNAs of *ECHDC1* and *ANKH* in ONFH.

Our research firstly investigated the function of identified RNAs in ONFH development through mRNAs-miRNAs-lncRNAs ceRNA network. Moreover, newly identified lncRNA *C9orf163* was first identified and validated as a key lncRNA in the progress of ONFH.

Nevertheless, our study has several limitations. First, our ONFH sample size for analysis was small. Second, most of the differentially expressed lncRNAs and mRNAs still need validation. Finally, although the ceRNA network of lncRNAs and mRNAs were constructed, the mechanisms of these lncRNAs and mRNAs need to be further investigated.

Conclusion

Based on our analysis, a total of 28, 1403, and 134 DE-lncRNAs, DE-mRNAs, and DE-miRNAs were identified respectively. The differentially expressed mRNAs were enriched in "skeletal system development," "collagen fibril organization," "blood vessel development," and "regulation of nervous system development." Seventy-two KEGG pathways were identified including eight active pathways and 64 inactive pathways, including which immune pathway is significantly activated and which ribosome-related function was mostly inhibited. The ceRNA network indicated that lncRNA *H19* might bind both hsa-miR-519b-3p and hsa-miR-296-5p, then *ECHDC1* and *ANKH* were up-regulated. LncRNA *c9orf163* could up-regulate *CCNT1* by targeting hsa-miR-424-5p.

An Authorship Declaration

All authors listed meet the authorship criteria according to the latest guidelines of the International Committee of Medical Journal Editors, and all authors are in agreement with the manuscript.

Supporting Information

Additional Supporting Information may be found in the online version of this article on the publisher's web-site:

Table S1. The top 10 suppressed pathways and the eight activated pathways.

References

1. Mont MA, Cherian JJ, Sierra RJ, et al. Nontraumatic osteonecrosis of the femoral head: where do we stand today? A ten-year update. J Bone Joint Surg Am, 2015, 97: 1604–1627.
2. Choi HR, Steinberg ME. E YC. Osteonecrosis of the femoral head: diagnosis and classification systems. Curr rev. Musculoskeletal Med, 2015, 8: 210–220.
3. Goyal T, Singh A, Sharma R, et al. Osteo-necrosis of femoral head in north Indian population: risk factors and clinico-radiological correlation. Clin Epidemiol Glob Health, 2019, 7: 446–449.
4. Wang G, Zhang C, Sun Y, et al. Changes in femoral head blood supply and vascular endothelial growth factor in rabbits with steroid-induced osteonecrosis. J Int Med Res, 2010, 38: 1060–1069.

5. Zheng L, Wang W, Ni J, et al. Plasma interleukin 33 level in patients with osteonecrosis of femoral head: an Alarmin for osteonecrosis of the femoral head? J Investig Med, 2014, 62: 635–637.
6. Wang Q, Yang Q, Chen G, et al. LncRNA expression profiling of BMSCs in osteonecrosis of the femoral head associated with increased adipogenic and decreased osteogenic differentiation. Sci Rep, 2018, 8: 9127.
7. Xiang S, Li Z, Weng X. The role of lncRNA RP11-154D6 in steroid-induced osteonecrosis of the femoral head through BMSC regulation. J Cell Biochem, 2019, 120: 18435–18445.
8. Huang G, Zhao G, Xia J, et al. FGF2 and FAM201A affect the development of osteonecrosis of the femoral head after femoral neck fracture. Gene, 2018, 652: 39–47.

CERNA NETWORK IN ONFH

9. Chen X, Li J, Liang D, et al. LncRNA AWPPH participates in the development of non-traumatic osteonecrosis of femoral head by upregulating Runx2. Exp Ther Med, 2020, 19: 153–159.

10. Kumar V, Westra HJ, Karjalainen J, et al. Human disease-associated genetic variation impacts large intergenic non-coding RNA expression. PLoS Genet, 2013, 9: e1003201.

11. Ha M, Kim VN. Regulation of microRNA biogenesis. Nat Rev Mol Cell Biol, 2014, 15: 509–524.

12. Ji X, Chen X, Yu X. MicroRNAs in Osteoclastogenesis and function: potential therapeutic targets for osteoporosis. Int J Mol Sci, 2016, 17: 349.

13. Li Z, Shen J, Chan MT, et al. MicroRNA-379 suppresses osteosarcoma progression by targeting PDK1. J Cell Mol Med, 2017, 21: 315–323.

14. Xu JF, Zhang SJ, Zhao C, et al. Altered microRNA expression profile in synovial fluid from patients with knee osteoarthritis with treatment of hyaluronic acid. Mol Diagn Ther, 2015, 19: 299–308.

15. Yu X, Li Z, Shen J, et al. MicroRNA-10b promotes nucleus pulposus cell proliferation through RhoC-Akt pathway by targeting HOXD10 in intervertebral disc degeneration. PLoS One, 2013, 8: e83080.

16. Wu X, Zhang Y, Xiong G, et al. Identification of differentially expressed microRNAs involved in non-traumatic osteonecrosis through microRNA expression profiling. Gene, 2015, 565: 22–29.

17. Wei B, Wei W. Identification of aberrantly expressed of serum microRNAs in patients with hormone-induced non-traumatic osteonecrosis of the femoral head. Biomed Pharmacother, 2015, 75: 191–195.

18. Yuan HF, Von Roemeling C, Gao HD, et al. Analysis of altered microRNA expression profile in the reparative interface of the femoral head with osteonecrosis. Exp Mol Pathol, 2015, 98: 158–163.

19. Bian Y, Qian W, Li H, et al. Pathogenesis of glucocorticoid-induced avascular necrosis: a microarray analysis of gene expression in vitro. Int J Mol Med, 2015, 36: 678–684.

20. Fatica A, Bozzoni I. Long non-coding RNAs: new players in cell differentiation and development. Nat Rev Genet, 2014, 15: 7–21.

21. Wei B, Wei W, Zhao B, et al. Long non-coding RNA HOTAIR inhibits miR-17-5p to regulate osteogenic differentiation and proliferation in non-traumatic osteonecrosis of femoral head. PLoS One, 2017, 12: e0169097.

22. Xiong DD, Li ZY, Liang L, et al. The LncRNA NEAT1 accelerates lung adenocarcinoma deterioration and binds to Mir-193a-3p as a competitive endogenous RNA. Cell Physiol Biochem, 2018, 48: 905–918.

23. Barrett T, Wilhite SE, Ledoux P, et al. NCBI GEO: archive for functional genomics data sets—update. Nucleic Acids Res., 2013, 41: D991–D995.

24. Liu R, Liu Q, Wang K, et al. Comparative analysis of gene expression profiles in normal hip human cartilage and cartilage from patients with necrosis of the femoral head. Arthritis Res Ther, 2016, 18: 98.

25. Cavallini A, Rotelli MT, Lippolis C, et al. Human microRNA expression in sporadic and FAP-associated desmoid tumors and correlation with beta-catenin mutations. Oncotarget, 2017, 8: 41866–41875.

26. Li T, Zhang Y, Wang R, et al. Discovery and validation an eight-biomarker serum gene signature for the diagnosis of steroid-induced osteonecrosis of the femoral head. Bone, 2019, 122: 199–208.

27. Ritchie ME, Phipson B, Wu D, et al. Limma powers differential expression analyses for RNA-sequencing and microarray studies. Nucleic Acids Res, 2015, 43: e47.

28. Huang d W, Sherman BT, Lempicki RA. Systematic and integrative analysis of large gene lists using DAVID bioinformatics resources. Nat Protoc, 2009, 4: 44–57.

29. Kanehisa M, Goto SKEGG. Kyoto encyclopedia of genes and genomes. Nucleic Acids Res, 2000, 28: 27–30.

30. Shannon P, Markiel A, Ozier O, et al. Cytoscape: a software environment for integrated models of biomolecular interaction networks. Genome Res, 2003, 13: 2498–2504.

31. Li JH, Liu S, Zhou H, et al. starBase v2.0: decoding miRNA-ceRNA, miRNA-ncRNA and protein-RNA interaction networks from large-scale CLIP-Seq data. Nucleic Acids Res, 2014, 42: D92–D97.

32. Wang GJ, Sweet DE, Reger SI, et al. Fat-cell changes as a mechanism of avascular necrosis of the femoral head in cortisone-treated rabbits. J Bone Joint Surg Am, 1977, 59: 729–735.

33. Wang T, Azeddine B, Mah W, et al. Osteonecrosis of the femoral head: genetic basis. Int Orthop, 2019, 43: 519–530.

34. Samara S, Kollia P, Dailiana Z, et al. Predictive role of cytokine gene polymorphisms for the development of femoral head osteonecrosis. Dis Markers, 2012, 33: 215–221.

35. Oppmann B, Lesley R, Blom B, et al. Novel p19 protein engages IL-12p40 to form a cytokine, IL-23, with biological activities similar as well as distinct from IL-12. Immunity, 2000, 13: 715–725.

36. Parham C, Chirica M, Timans J, et al. A receptor for the heterodimeric cytokine IL-23 is composed of IL-12Rbeta1 and a novel cytokine receptor subunit, IL-23R. J Immunol, 2002, 168: 5699–5708.

37. El-Tahan RR, Ghoneim AM, El-Mashad N. TNF-alpha gene polymorphisms and expression. Springerplus, 2016, 5: 1508.

38. Hao C, Yang S, Xu W, et al. MiR-708 promotes steroid-induced osteonecrosis of femoral head, suppresses osteogenic differentiation by targeting SMAD3. Sci Rep, 2016, 6: 22599.

39. Yuan HF, Christina VR, Guo CA, et al. Involvement of MicroRNA-210 Demethylation in steroid-associated osteonecrosis of the femoral head. Sci Rep, 2016, 6: 20046.

40. Jia J, Feng X, Xu W, et al. MiR-17-5p modulates osteoblastic differentiation and cell proliferation by targeting SMAD7 in non-traumatic osteonecrosis. Exp Mol Med, 2014, 46: e107.

41. Sun J, Wang Y, Li Y, et al. Downregulation of PPARgamma by miR-548d-5p suppresses the adipogenic differentiation of human bone marrow mesenchymal stem cells and enhances their osteogenic potential. J Transl Med, 2014, 12: 168.

42. Fang B, Li Y, Chen C, et al. Huo Xue Tong Luo capsule ameliorates osteonecrosis of femoral head through inhibiting lncRNA-Miat. J Ethnopharmacol, 2019, 111862: 238.

43. Yamaguchi R, Yamamoto T, Motomura G, et al. Incidence of nontraumatic osteonecrosis of the femoral head in the Japanese population. Arthritis Rheum, 2011, 63: 3169–3173.

44. Igarashi M, Hayashi Y, Karube S, et al. An aspect of metabolic bone disease with idiopathic osteonecrosis of the femoral head. Nihon Seikeigeka Gakkai Zasshi, 1983, 57: 379–384.

45. Yoshimura H, Matsuda Y, Yamamoto M, et al. Expression and role of long non-coding RNA H19 in carcinogenesis. Front Biosci, 2018, 23: 614–625.

46. Xu C, Li S, Chen T, et al. miR-296-5p suppresses cell viability by directly targeting PLK1 in non-small cell lung cancer. Oncol Rep, 2016, 35: 497–503.

47. Connolly M, Paul R, Farre-Garros R, et al. miR-424-5p reduces ribosomal RNA and protein synthesis in muscle wasting. J Cachexia Sarcopenia Muscle, 2018, 9: 400–416.

48. Zhang Y, Sun M, Chen Y, et al. MiR-519b-3p inhibits the proliferation and invasion in colorectal cancer via modulating the uMtCK/Wnt signaling pathway. Front Pharmacol, 2019, 10: 741.

49. Zhuang Q, Ye B, Hui S, et al. Long noncoding RNA lncAIS downregulation in mesenchymal stem cells is implicated in the pathogenesis of adolescent idiopathic scoliosis. Cell Death Differ, 2019, 26: 1700–1715.

50. Abhishek A, Doherty M. Pathophysiology of articular chondrocalcinosis: role of ANKH. Nat Rev Rheumatol, 2011, 7: 96–104.